5-1-2020

ECCENTRIC ROTATING MASS MOTOR VIBRATIONAL PLATE MODELING

Lukas Willingham

ECCENTRIC ROTATING MASS MOTOR VIBRATIONAL PLATE MODELING

by

LUKAS TYLER WILLINGHAM

Presented to the Faculty of the Honors College of

The University of Texas at Arlington in Partial Fulfillment

of the Requirements

for the Degree of

HONORS BACHELOR OF SCIENCE IN MECHANICAL ENGINEERING

THE UNIVERSITY OF TEXAS AT ARLINGTON

May 2020

ACKNOWLEDGMENTS

First and foremost, I would like to thank my wife, Samantha Willingham, for her endless support throughout my college career as well as sparking this change in career path. She saw that I was miserable in a job that I didn't enjoy and she pushed me to see what my career could be like in Engineering. Without her sacrifices I wouldn't be anywhere near where I am today. She pushes me to believe that I am capable of greater things than I ever imagined and provides me with someone that I can look up to in every moment of my life.

I would also like to thank my Pulse Engineering teammates for this project: Kelly Johnson, Jason Alford, Joseph Wyatt and Brandi Garland. They were always open-minded when I got an idea that I wanted to run with and always were willing to see an idea through. Their suggestions and input made both this project and the full Senior Design group project a wonderful experience and one that we can all be proud of.

Finally, I want to thank the professors of the University of Texas at Arlington: most notably Dr. Raul Fernandez, Dr. Adrian Rodriguez and Dr. Nancy Michael. This career path is not one that I picked lightly and they did not shy away from the difficulty of a profession within STEM. However, the passion that they showed in their chosen field reflects why all of us picked Engineering in the first place.

April 14, 2020

ABSTRACT

ECCENTRIC ROTATING MASS MOTOR

VIBRATIONAL PLATE MODELING

Lukas Willingham, B.S. Mechanical Engineering

The University of Texas at Arlington, 2020

Faculty Mentor: Dr. Raul Fernandez

To design and analyze a vibrational plate design, multiple steps must be followed to find the time response of the system. The design was created using an existing patent for the design objectives and the technology that must be avoided. The design was then created using a Delrin plastic sheet, a set of springs, 4 linearization bearings and a vibrational motor. From this point a Free-Body Diagram was set up to find the governing equations of the system. Using these equations, the time response was found using two different numerical methods: the ODE45 program within MATLAB and Laplace/Inverse Laplace. Using ODE45, the displacement of the vibrational sheet was found and using this result, various parameters were adjusted to reach a displacement of 0.1-0.2-inches. These parameters include the number of springs, the spring constant and the size of the eccentric mass. With these parameters in place, the ODE45 time response was found to be 0.25 inches for a user of 188lbs.

When the same system is analyzed using the Laplace and Inverse Laplace by hand method, the displacement was found to be 0.26 inches. This represents a 6% difference in the results of the two methods. For this application that only shows a 0.01-inch difference. These two solutions represent effectively equal results.

TABLE OF CONTENTS

LIST OF ILLUSTRATIONS

LIST OF TABLES

CHAPTER 1

INTRODUCTION

1.1 Background

The world has become an increasingly stimulating and chaotic place. The connection between the human experience and the advertising world has become almost synonymous. This is not to mention the connection the world has to technical devices that simplify the majority of life and make information available at the fingertips of the user. However, these devices increase the over-stimulation of the auditory and visual parts of the brain. Numerous industries have been created as a way to combat this stimulation. Products such as noise-canceling headphones and sensory deprivation tanks push towards this goal. These products try to provide relief through either flooding the user with audio to drown out the outside world or to remove everything and leave the user with total silence. These different types of stimuli can lead instead to an increase in stress and keeps the user focused on the issues they are trying to remove themselves from. The use of meditation and relaxation is used to relieve the external focus to calm the mind and counter stress and stress-related ailments. Meditation and a sense of relaxation have caused benefits across the medical field by curing insomnia, lowering depression and stress, reducing blood pressure, and relieving some effects of autism. [Stress Management. (n.d.)]

To fully achieve relaxation in a time of overstimulation, the user must find awareness of the body. This awareness is typically only realized during times of discomfort or pain.

One way to achieve this awareness is by increasing the stimulation to the body so the perception of the stimulus is also increased. This increased stimulation is called vibration therapy. This stimulation can be heightened by the use of music therapy, or sound therapy. The combination of vibration and sound therapy allows for the user to be fully immersed and allows the brain to calm and reach the levels of meditation and relaxation needed to provide health benefits to the user.

1.2 Client Request

The client, Science-Based Mind and Body (SBMB), came to Pulse Engineering with a vibrational/sound therapy chair that is currently in production and patent protected. They were looking to receive outputs of a similar, or better, nature to that of the SolTec Lounge. However, since the SolTec Lounge is a patent-protected design, SBMB was also looking to achieve intellectual property on a separate design to avoid licensing fees. The SolTec Lounge uses mass and cone transducers (similar to a speaker) to provide the vibration to the user. To achieve this intellectual property, several different types of vibrational systems were researched to find a suitable replacement. The vibration sources that Pulse Engineering researched include eccentric rotating mass motors, linear resonant actuators, a rotating fluid reserve and linear post actuators. The primary source of vibration researched was the use of eccentric rotating mass motors. Since SBMB is a company of only two, several considerations had to be considered: mass production versus off the shelf parts, price comparison to the SolTec Lounge, environmental effects of materials, and variation of design for different environments.

1.3 Eccentric Rotating Mass Motors

Eccentric rotating mass (ERM) motors are most commonly found within the use of cell phones and video game controllers as a way to provide tactile feedback to the user. This tactile feedback is provided through the vibration of the entire motor unit. These motors create vibration through use of a spinning mass that is either asymmetrical or attached to a shaft in a position other than that of the center of mass for the eccentric mass. Figure 1.1 shows typical eccentric mass designs along with the center of mass for each. This distance between the rotation point, the shaft of the motor, and the center of mass for the rotating body provides centrifugal force in the direction of the center of mass which provides a vibration.

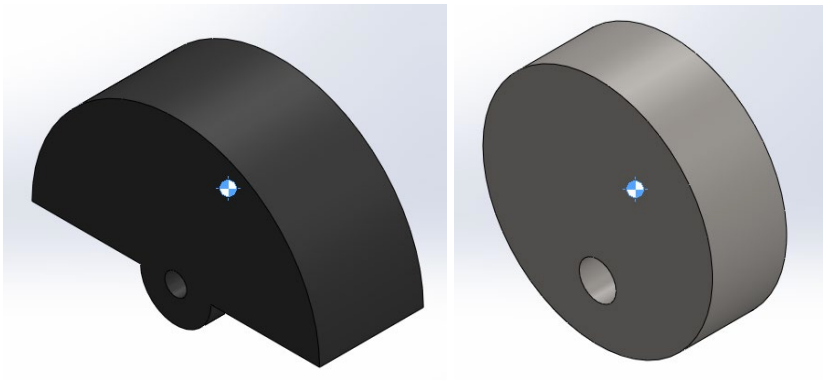

Figure 1.1: Eccentric Mass with the Center of Mass

The produced force is a function of the eccentricity [e] (the distance between the center of mass and the shaft of the motor), the angular velocity of the motor, and the mass of the eccentric body. This force can be calculated using Eq.(1). As this equation shows, for a rotating body, the mass and eccentricity are fixed once the geometry and material are chosen, this leaves the angular velocity as a key variable for the force output of the

vibrational motor. This velocity can be controlled using the RPM rating of a motor and using Eq.(2) to find the needed angular velocity for a required output force.

$$F_o = mr\omega^2 \quad \text{Eq.(1)}$$

$$\omega = \frac{2\pi * RPM}{60} \quad \text{Eq.(2)}$$

$$F = F_o \sin(\omega t) \quad \text{Eq.(3)}$$

As previously mentioned, the force produced by the motor acts in the direction of the center of mass of the rotating body. Because the vibrational amplitude needed to be analyzed in only the y-direction, this force must be linearized. To do this, the force needed to be treated as the peak amplitude for a sinusoidal input. This relationship is given by the projection of a point in a circular motion onto a single set of X/Y axes and can be seen in Figure 1.2. With this linearization the force output of the ERM motor is calculated using Eq.(3).

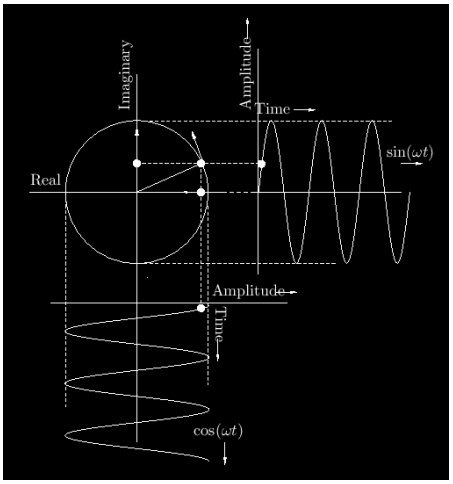

Figure 1.2: Relating Circular Motion to Sinusoidal Motion (J.O. Smith, 2007)

1.4 Free Body Diagram Approach

Following the initial idea design of the body, the calculation of forces must be compared and analyzed for balance and motion. This is done by the drawing and analysis of a free-body diagram (FBD). FBD's show the general shape of the body in question and show each of the forces and moments that act upon it. These forces and moments are then summed to equal zero concerning Newton's Laws of Motion. The equations relating to these ideas can be found in Eq.(4) and (5).

$$\sum F_{x,y,z} = ma_{x,y,z} = 0 \qquad \text{Eq.(4)}$$

$$\sum M_{x,y,z} = I_{x,y,z}\alpha_{x,y,z} = 0 \qquad \text{Eq.(5)}$$

Typical elements found within these FBD's include simple applied forces, gravitational force, springs, dampers and the force due to D'Alembert's principle. D'Alembert's Principle is an extension of Newton's Second Law of Motion which pulls the "ma" term to the left side of the equation resulting in Eq.(6). This "ma" term will act in the opposite direction of motion for the body and acts as another force input to the system. The equation for spring forces, damper forces, and gravitational forces are given in Eq.(7)-(9) respectively.

$$\sum F_{x,y,z} - ma_{x,y,z} = 0 \qquad \text{Eq.(6)}$$

$$F_s = ky \qquad \text{Eq.(7)}$$

$$F_d = b\dot{y} \qquad \text{Eq.(8)}$$

$$F_g = ma = m\ddot{y} \qquad \text{Eq.(9)}$$

Let us look at the simple diagram in Figure 1.4.1 and Figure 1.4.2. Here a simple mass (M) is moving in the positive y-direction with a spring and damper acting upon it. Once the original FBD from Figure 1.3 is broken apart to analyze the individual forces acting upon it, the diagram in Figure 1.4 can be drawn. From this diagram a force balance is done on each body (the mass, the spring and the damper). The equations found in Eq.(10-13) are extracted.

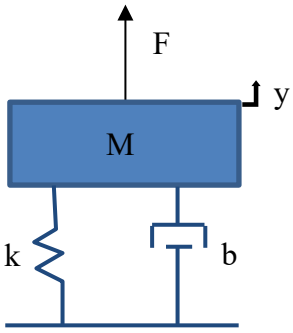

Figure 1.3: Body for Analysis

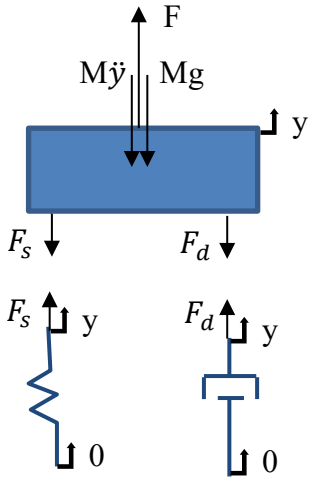

Figure 1.4: Each Body is Separated to Analyze Each Force

$$F_s = k(y - 0) = ky \qquad \text{Eq.(10)}$$

$$F_d = b(\dot{y} - 0) = b\dot{y} \qquad \text{Eq.(11)}$$

$$M\ddot{y} + Mg + F_s + F_d = F \qquad \text{Eq.(12)}$$

$$M\ddot{y} + b\dot{y} + ky + Mg = F \qquad \text{Eq.(13)}$$

From this point, further examination is required. The solution of an ordinary differential equation is needed. To serve this purpose, the Laplace Transform and the Inverse Laplace Transform must be used.

1.5 Laplace and Inverse Laplace Transform

The Laplace/Inverse Laplace transform is one of many ways to solve an ordinary differential equation for the time domain solution/response of the system. This provides a way for researchers to analyze the expected time response of a differential equation that is the output of the free body diagram formation and analysis. As seen in Eq.(13), this equation not only possesses the position (y) but also the first and second derivative of the position, the velocity and acceleration in the y-direction. To solve for only the position response of the system, manipulation must be performed by way of the Laplace Transform.

1.5.1 Laplace Transform

The Laplace Transform is defined by the use of Eq. (14). In this equation f(t) is a function of time (similar to Eq.(13)) and F(s) is the transformed function in the Laplace domain. The Laplace operator (s) becomes the dominating variable in the function.

$$\mathcal{L}(f(t)) = F(s) = \int_{0^-}^{\infty} f(t)e^{-st}dt \qquad \text{Eq.(14)}$$

There are a few Laplace identities that must be considered, the Laplace of a constant, a sinusoid, and a derivative. The Laplace function of a constant, u, is equal to that constant over the Laplace operator (u/s). For a sinusoidal input ($\sin(wt)$), the Laplace transform is $\frac{w}{s^2+w^2}$. If this sinusoid is multiplied by a constant value ($A\sin(wt)$), then the Laplace transform of the sinusoid is also multiplied by that constant ($\frac{Aw}{s^2+w^2}$). Finally, for a derivative of a time function the Laplace transform is given by Eq.(15-17).

$$\mathcal{L}\left(\frac{d^n f}{dt^n}\right) = s^n F(s) - \sum_{k=1}^{n} s^{n-k} f^{k-1}(0-) \quad \text{Eq.(15)}$$

$$\mathcal{L}\left(\frac{df}{dt}\right) = sF(s) - f(0-) \quad \text{Eq.(16)}$$

$$\mathcal{L}\left(\frac{d^2 f}{dt^2}\right) = s^2 F(s) - sf(0-) - f'(0-) \quad \text{Eq.(17)}$$

In these equations, f(0-) represents the initial value of the original function (in our case, the y function) and f'(0-) represents the initial value of the derivative of this function, in our case, the velocity. To apply these identities to our earlier example, the Laplace of Eq.(13) becomes Eq.(18-19). One thing to note is that if the initial conditions are zero for either the f'(0-) or f(0-) case then this form simplifies further. The final simplified form of Eq.(19) is known as the transfer function of the system and is the basis of how this function transfers to the Laplace domain.

$$M(s^2 Y(s) - sy(0-) - \dot{y}(0-)) + b(sY(s) - y(0-)) + kY(s) + \frac{Mg}{s} = \frac{F}{s} \quad \text{Eq.(18)}$$

$$F(s) = Y(s) = \frac{My(0-)s^2 + \left(M\dot{y}(0-) + by(0-)\right)s - Mg + F}{Ms^3 + bs^2 + ks} \quad \text{Eq.(19)}$$

From this transfer function, the next step to solve this equation by hand is to use the Inverse Laplace Transform to place it back in the time domain.

1.5.2 Inverse Laplace Transform

The Inverse Laplace Transform is defined by Eq.(20) and is used to transform the Laplace domain solution back into the time domain to find the function for the y response of the system.

$$\mathcal{L}^{-1}[F(s)] = \frac{1}{2\pi j}\int_{\sigma-j\infty}^{\sigma+j\infty} F(s)e^{st}ds = f(t) \qquad \text{Eq.(20)}$$

Using the reverse of the identities previously discussed while discussing Laplace Transforms of typical forms along with a few additional Laplace transforms we can find this Inverse Laplace Form. One Laplace transform that will be useful is the Laplace of e^{-at} being equal to $\frac{1}{s+a}$. This allows us to use partial fraction decomposition from a transfer function to provide a time-domain solution.

Using our previous example, if we assume that the initial value for velocity is equal to zero and we find that the initial value of y = $\frac{-Mg}{k}$. If we also assume values for F, m, k and b to be 40 lb, 6 lb, 10 lb/ft and 16 lb*s/ft, respectively. In this case, Eq.(19) becomes Eq.(21) and simplifies as shown.

$$Y(s) = \frac{-115.8s^2 - 308.8s - 153.044}{6s^3 + 16s^2 + 10s} = \frac{-91.83}{s} + \frac{-59.99}{s+1} + \frac{35.99}{s+\frac{5}{3}} \qquad \text{Eq.(21)}$$

Using this simplified form and the identities previously discussed the time domain function can be extracted as Eq.(22).

$$y(t) = -91.83 - 59.99e^{-t} + 35.99e^{-\frac{5}{3}t} \qquad \text{Eq.(22)}$$

This response can also be extracted in graphical format by use of MATLAB programming and the ODE45 function. While the response can be viewed within the MATLAB program, the final closed-form solution (seen in Eq.(22)) cannot be extracted using ODE45.

1.6 ODE45

The response of this time-domain solution can be extracted from the transfer function of the Laplace domain by use of the ODE45 function within MATLAB. This MATLAB function uses the Runge-Kutta method of solving differential equations, using a few initial conditions, to produce a visual representation of the variable in question over time. To use ODE45, the equations of the system must be placed into a state-variable format. State-variable format provides a simple translation to the coding language used by the MATLAB software. In this format, each variable is placed into a matrix of values, x(1) = y, x(2) = y', etc. There will be a set of, in this case, x variables and a set of d/dt values for the same set (using x(1) and x(2) where applicable). Using our previous example as a test-case, Eq.(23)-(25) becomes our set of state variable equations.

$$x(1) = y \qquad \text{Eq.(23)}$$

$$x(2) = \frac{dx(1)}{dt} \qquad \text{Eq.(24)}$$

$$\frac{dx(2)}{dt} = -g - \frac{kx(1)}{M} - \frac{bx(2)}{M} + \frac{F}{M} \qquad \text{Eq.(25)}$$

When coding, the line that calls the function of ODE45 is [t,y] = ode45(@eqns, [tspan] [yo]). In this line of code, @eqns is the function in which a y-matrix of zeros is created (dy = zeros(2,1)) which takes the y' and y'' values. This function is also what collects the state-

variable formulas that were previously discussed. Tspan is the period that you want ode45 to run the set of equations and yo is the set of initial values present in the equation set.

Once the ode45 code is complete with the @eqns function complete, the user must isolate which variable is of interest in plotting. In our current example, we are analyzing the y displacement of the mass. Therefore, y(:,1) is the variable of interest. When ode45 is run for this example problem, the system response seen in Figure 1.5 is extracted. The MATLAB code for this example, along with the hand calculations for the previous steps, can be found in Appendix A.

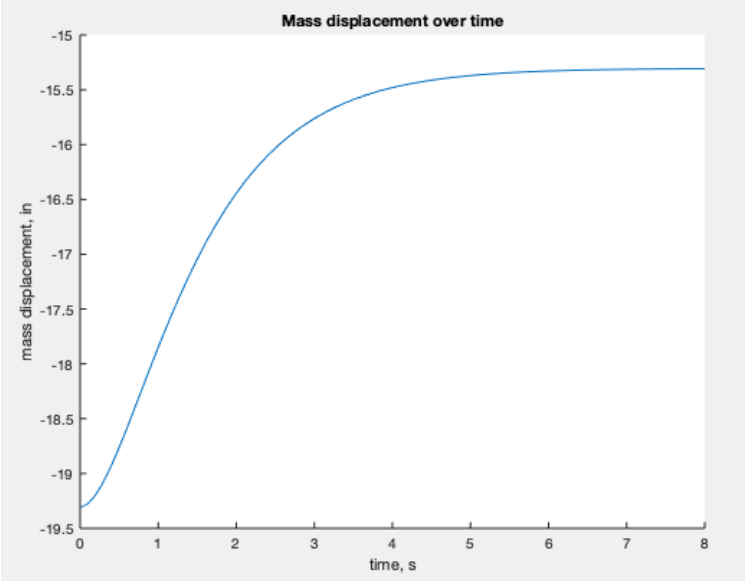

Figure 1.5: Mass Displacement Over Time

CHAPTER 2

LITERATURE REVIEW

2.1 Previous Patents

When attacking the vibrational plate problem, the focus of Pulse Engineering was the main functionality of the chair/plate. This has narrowed the scope of the literature review to the existing patents for a few products that are similar in purpose and function: the SolTec Lounge and the SoSound collection of loungers. While other vibration inventions exist, due to the purpose of this product, those will not be expounded upon here unless they possess a clear connection to the use and design of the Pulse Engineering vibrational platform.

2.1.1 SolTec Lounge

The SolTec Lounge is the product that was presented to Pulse Engineering as the basis of the design project at hand. The SolTec Lounge is detailed under patent number US 9,949,004 B2 entitled "Sound and Vibration Transmission Device" dated April 17, 2018. This patent details the sound and vibration transmitting apparatus by the use of transducers that are coupled to a frame made to support at least part of a user's body. The frames specified in this patent include chairs, beds and pads. The transducer is also meant to produce an electromagnetic field large enough to provide stimulation to the user. These transducers are coupled to a chair and set up in a way as to transfer vibration through the seat and the back of the user. The setup of these transducers can be seen in Figure 2.1.

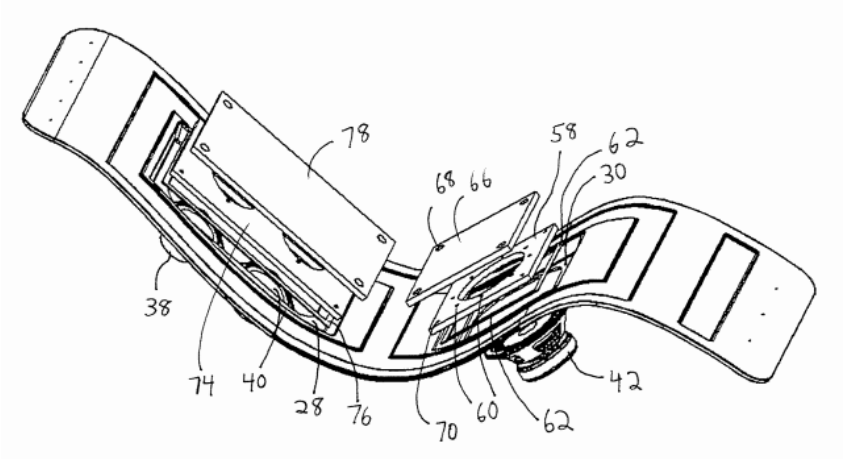

Figure 2.1: Layout of SolTec Vibrational Plates within a Lounger
(U.S. Patent No. 9,949,004, 2018)

The transducers for the SolTec Lounge are comprised of a mass-loaded cone, similar to that of a speaker. The main difference between a mass-loaded cone transducer and the type used as a speaker is the weight of the cone. For a sound-producing transducer, the cone is lightweight and produced mostly out of paper or plastic. The mass-loaded cone transducer has a much heavier cone attached rigidly to a structure as a way to impart a larger vibrational force to the structure itself. It is also claimed that this transducer is capable of translating 0.1-0.2 inches about the frame of the structure. This translation/displacement is said to be "in a direction parallel to the movement of the mass-loaded cone" (U.S. Patent No. 9,949,004, 2018). This means that the displacement of 0.1-0.2 inches is considered in the direction of the user. The vibration produced by the transducer is stated to be between 0.5-1000 Hz.

The purpose of this invention was to provide health benefits to the user by a device and method for the administering of sound and vibrational therapy. The vibration of the body is meant to vibratethe organs of the user’s body and could be tailored to target a specific organ by use of frequency modulation.

2.1.2 SoSound Loungers

The SoSound company is one that uses vibrational technology within loungers/chairs as well as selling products aimed at retrofitting current chair designs with their patented transducer package. The transducers that SoSound uses are detailed under US Patent Number US 8,077,884 B2 entitled “Actuation of Floor Systems Using Mechanical and Electro-Active Polymer Transducers” from December 13, 2011. The patent details the befits of this type of technology, like the SolTec Patent detailed in section 2.1.1, and discusses various uses from flooring to bed integration.

This product is meant to transfer the sound energy from music to a person's body to help alleviate stress and calm the mind. They do this through the use of transducers placed within chairs, pillows, beds, and flooring. The transducer in use for the SoSound patent (and the product that is sold to retrofit current chairs/beds) can be placed into the coil spring of the chair or bed. This diaphragm and transducer can be seen in Figure 2.2.

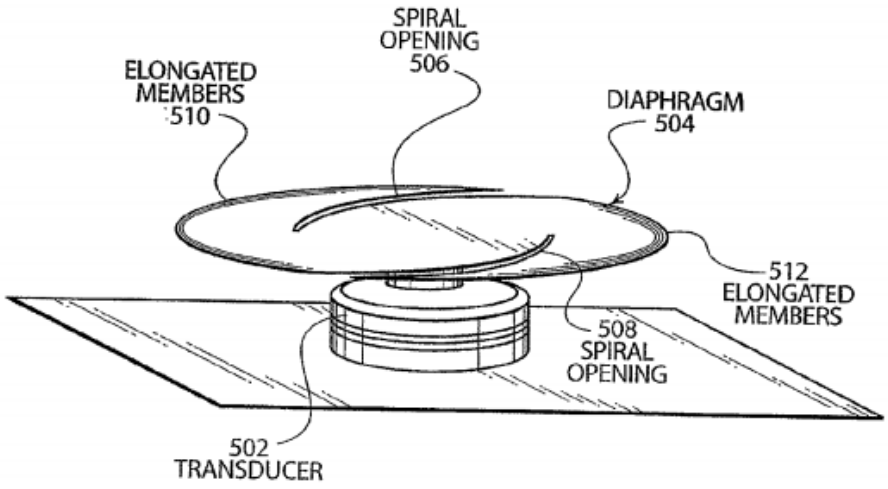

Figure 2.2: SoSound Diaphragm and Transducer
(U.S. Patent No. 8,077,884, 2011)

These transducers consist of a spinning diaphragm with a spiral cut and is elongated along the edges to shift the center of mass of the sheet. This shift of the center of mass away from the rotational center causes a “wobble” creating vibrational energy. When this transducer is placed within the coil spring of an existing chair or bed it is seated as seen in Figure 2.3.

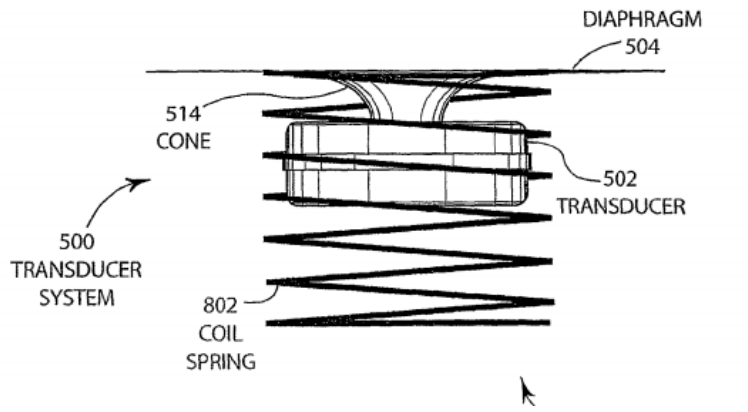

Figure 2.3: SoSound Transducer Seated Within Existing Spring
(U.S. Patent No. 8,077,884, 2011)

This patent resembles that of the Eccentric Rotating Mass motor, however, the geometry and cut of the rotating disc categorize this as a different type of vibrational source entirely.

CHAPTER 3

METHODOLOGY

The starting point for this experiment was the data extracted from the patent review. The mass-cone transducer could not be used but a displacement of 0.1-0.2 inches needed to be achieved. Due to this limitation, a new form of vibration needed to be discovered. This led to an exploration of various vibrational sources: the ERM motor, a Linear Resonant Actuator, a rotating fluid reserve, and a linear actuating motor. Each vibrational source was researched for cost, weight, vibrational output, and availability. Once a vibrational source was chosen, a basic model would then be designed.

This basic model should consist of some combination of a simple plate, the vibrational source, along with a mix of springs, dampers, and linearization posts (along with any necessary connecting materials). This design would be chosen for ease of build, cost of individual parts, and recyclability. After this, a free body diagram approach would be followed to find the governing equations of the systems and what parameters would need to be assigned. These parameters would be assigned to initial values to find the initial displacement of the system. These parameters could then be altered to find a combination that would achieve the necessary displacement. From this point, the equations will be in a differential equation form. The goal is to find the y-axis displacement for the vibrational system.

With this in mind, the ODE45 program within MATLAB will be used to solve the system for this y displacement. Once a sufficient displacement is found, the differential equation will be solved by hand for a specific weight of the user to find the equation of the displacement of the system.

CHAPTER 4

RESULTS AND DISCUSSION

To begin this project, the working knowledge that was gained from the literature resulted in two points: the mass-cone transducer could not be used and a displacement of a vibrational plate needed to be at least 0.1-0.2 inches. The first of these points would be the first thing addressed: what vibrational source will be able to create this type of vibration.

4.1 Vibrational Source

Several sources were initially considered. The points of comparison for each of these options were the vibrational output, the cost, and the availability of each option. The motors that were researched include the Linear Actuating Motor, a rotating fluid reserve, a Resonant Actuator, and the Eccentric Rotating Motor.

4.1.1 Linear Actuating Motors

The first of these was the use of linear actuating posts. A controller motor spins and pushes the post in or out of a linearizing housing. The rotational motion of the motor is converted to linear motion by the use of a set of gears and a worm gear. The internal parts of the linear actuating motor can be seen in Figure 4.1.

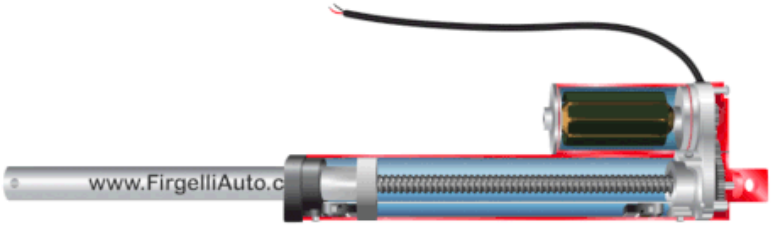

Figure 4.1: Linear Actuating Motor (Linear Actuators, 2018)

This option would provide a simplification to design because the LAM can only work in one direction. This would allow the design to not need any sort of linearization addition to the design. However, the large issue with this choice is the speed at which they can run. Due to the needs of the transition from rotational to linear, the speed of the linear motion will not be as large as the speed of rotation. Additionally, due to the need for a relatively small gearbox, this speed will be reduced. These difficulties remove the Linear Actuating Motor from the list of possibilities.

4.1.2 Rotating Fluid Reserve

The next possibility for a vibrational source is a rotating fluid reserve. This option consists of a closed fluid container that will spin with the use of a motor. The fluid tank can be added to or removed from to adjust the amount of force needed to displace the vibrational plate. This force would be calculated similarly to that of the ERM motor discussed in the Introduction. However, the issue with this type of vibrational source is the actual calculation of the force itself. As previously stated, the force of a rotating mass is a function of the distance between the rotational center (the rotational shaft) and the center of mass for the weight. In this case the rotating mass is a bank of fluid. The calculation of the shape of a rotating fluid is one that creates an extremely complex problem. Due to this issue and the fact this would have to be fully manufactured, the rotating fluid reserve was also removed from consideration.

4.1.3 Linear Resonant Actuator

The next option under consideration was the Linear Resonant Actuator (LRA). This is another vibrational source which simplifies the force into only one direction, simplifying the design in the future. Along with ERM motors, LRA motors are used within many cell

phone designs to provide haptic feedback to the user. These motors are also similar to the ERM in that the movement of the internal mass is what creates the force for the vibration. However, the LRA motor uses a voice coil, similar to those seen in speakers and mass-cone transducers, and a magnetic mass attached to a spring. The voice coil drives the mass and the spring pushes the mass back, creating the vibrational force. An LRA motor created by Precision Microdrives can be found in Figure 4.2.

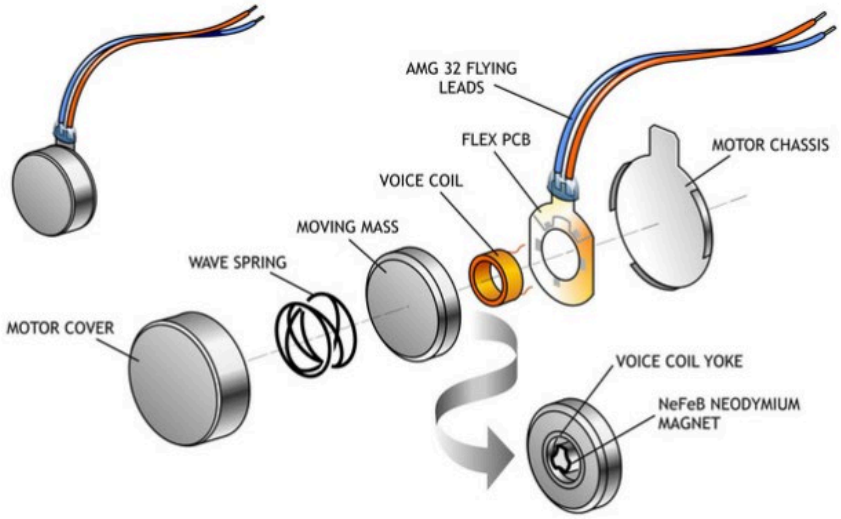

Figure 4.2 Precision Microdrive LRA (AB-020, n.d.)

However, the LRA motor has an issue of sizing. There are very few commercially available LRA motors that can produce the vibrational force that is necessary in this application. The lack of production can be explained by the existence of the mass-cone transducer. The workings are the same as the LRA and the sizing is much more scalable. So, even though this is considered a different type of motor from the mass-cone transducer, to scale it to the size that is needed in this application, the original patent would come into dispute.

4.1.4 Eccentric Rotating Mass

The final type of motor that was researched, and the motor that was chosen for use, was the Eccentric Rotating Motor. A review of the basics of the ERM motor can be found in the introduction. Within this application the strengths of this motor far surpass those of the other motors discussed. The ERM motor is commercially available in a multitude of sizes. The fact that the rotating mass itself makes the motor an ERM motor allows for most any rotational motor to be retrofitted with an eccentric mass. This opens up the sizing availability to any rotational motor. It is also available in a dual shaft configuration, allowing the minimization of space dedicated to the vibrational source. The vibrational force output can be chosen by the production of a larger or smaller eccentric mass. However, due to the directionality of the vibrational force, some form of linearization must be designed.

Once this type of motor was chosen, the next step in the design process was to create a simple design that could be created for analysis.

4.2 Basic Model Design and Free Body Diagram

A simple design was created using a plate, a set of springs, the ERM motor and a bottom plate. This design was created to be as simple as possible. A plate would transfer the vibrational energy from the motor. A set of springs would act as a translator for this energy as well. Finally, a group of bearing posts would help with the linearization of the system. Using these base design elements, a simple free body diagram (FBD) was created showing the forces acting on such a body. This FBD can be seen in Figure 4.3.

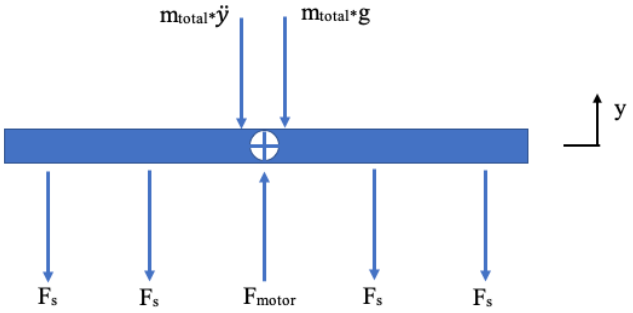

Figure 4.3: Initial Free Body Diagram of the System

This FBD considers the force input by the ERM motor, the force of the springs, the force due to gravity and the force due to d'Alembert's principle. The number of springs is shown as 4, however, this is only to show that there is a combination of springs within this design. Performing a force balance upon this FBD results in Eq (26). The M_{total} term of this equation is a combination of the mass of the entire system, including the user. The full summation of this term can be found in Eq.(27). The "pin" subscript coincides with the linearization bearing rods that will be used to keep the plate moving in only the y-direction.

$$m_{total}\ddot{y} + n_{springs}F_s + m_{total}g = F_{motor} \quad \text{Eq.(26)}$$

$$m_{total} = n_{pin} * (m_{pin} + m_{pinC}) + m_{sheet} + ((m_{motor} - n_{ecc} * m_{ecc} + m_{motorC})) + m_{user} \quad \text{Eq.(27)}$$

$$m_{total}\ddot{y} + n_{springs}ky + m_{total}g = n_{ecc}(m_{ecc}r\omega^2) * \sin(\omega t) \quad \text{Eq.(28)}$$

The "C" subscript refers to the hardware required to connect the parts to the plate (i.e. screws, connector plates etc.). Also included in this equation is a multiplier to adjust the number of springs within the design ($n_{springs}$) and the number of eccentric masses (n_{ecc}). Once the equation for the force of the springs and the equation for the force of the

motor is substituted in, the equation simplifies to Eq.(28). As discussed, due to the directionality of the force being created by the motor, the force must be linearized in the y-direction. This is done by taking the force of the motor as the amplitude of a sinusoidal input. From this point, a numerical problem-solving aid is needed.

4.3 ODE45

To solve the differential equation presented in Eq.(28), the ODE45 function within MATLAB is used to extract the displacement. Before writing this code, a few things must be assigned and found. The 12 parameters in this governing equation must be assigned before the displacement can be solved: the number of pins, the mass of the pins and the pin connectors, the mass of the plate/sheet, the mass of the motor and the motor connectors, the mass and eccentricity of the eccentric body, the RPM rating of the motor, the number of springs, the spring constant of those springs, and the mass of the user. All of these values are found by selecting parts through trial and error within the MATLAB code itself.

Four linearization bearing pins and connectors were chosen by my colleague, Jason Alford, and had masses of 0.05 lb and 0.0016 lb respectively. Four pins were chosen to be able to have one pin on each corner of the vibrational plate. This allows the distribution of stresses among the four pins which allows for each pin to be smaller in diameter. The vibrational plate was chosen to be Delrin due to the strength, low flexibility, and recyclability. This led to a plate mass of 0.0389 lb. The motor was chosen to be a Century 1/6 HP room air conditioner motor which has a dual shaft design. This motor comes with both the motor and the mounting hardware. With this in mind, the weight of the package (11.2 lb) is used as the weight of both the motor and mounting hardware. Due to this the

mass of the motor and the mass of the connectors are combined to 0.3481 lb. This motor also has a nameplate RPM of 1550 RPM.

The eccentric body is one of the two parts of this design that would be designed and manufactured for this build. The eccentric body was designed to be a circular mass weighing 2.1 lb each and having a center of mass 0.8 inches from the rotational center. Therefore, the mass of the eccentric body was found to be 0.0653 lb and the eccentricity was 0.0667 ft. The design of this mass can be seen in Figure 4.4. The number of springs was chosen to be 12. This allows for 3 springs on each side of the vibrational platform and distributes the weight of the system evenly around the perimeter of the plate. This number of springs also allows for smaller springs to save space along the outside of the vibrational plate. The spring constant was assigned an initial value of 15 lb/in. This spring constant would be adjusted later to help with vibrational speed (Hz) and the vibrational displacement.

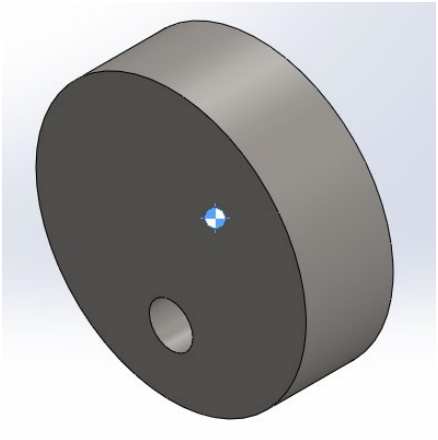

Figure 4.4: Eccentric Mass Design

Finally, the weight of the user was taken to be the US average from the Centers for Disease Control and Prevention of 188 lb. [Fryar (2018)]. Therefore, the mass of the user was found to be 4.5577 lb. However, because this plate will be placed in the seat of a chair,

a percentage of the bodyweight of the user must be found that is felt by the seat. To do this, a crude experiment was performed by standing on a common bathroom scale and then sitting on the same scale (within the seat of a chair). This experiment showed that 78% of the user's weight/mass is distributed to the seat of the chair.

With all of these parameters in place, an initial displacement run was performed for a time of 4 seconds. The performance of this run can be found in Figure 4.5. The displacement of the vibrational plate was found to be 0.382 inches and an initial displacement of 0.8652 inches in the negative y-direction. The vibrational speed was found to be roughly 3 Hz. This vibrational speed was judged as far too slow to feel a "vibration" instead of a slow tap from the plate.

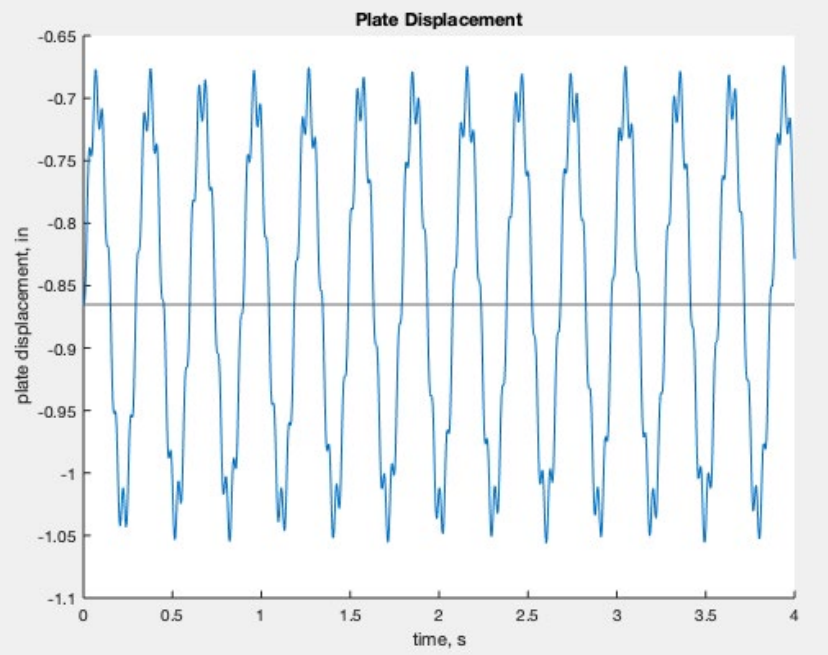

Figure 4.5: Initial run of k=15 lb/in

With all other parameters held constant, the spring constant was adjusted. The k value was increased steadily and a few correlations were noticed. The larger the k-value

the lower the displacement but the higher the vibrational Hz. With the previous run being 0.182 inches over the 0.2-inch baseline, there was room to increase the k-value and subsequently the vibrational speed. The other correlation that is noticed is that the higher the k-value of the spring, the lower the initial displacement of the system. This relationship is expected due to the definition of the spring constant. The k-value relates to the amount of force from the spring as the spring is compressed (or extended). For example, for a spring constant of 15 lb/in and an initial displacement of -0.8652 relates to a force of 17.34 lb per spring.

The k-value was finally increased to 46.1 lb/in. This value was chosen based on the availability of McMaster-Carr (mcmaster.com). The time response of this problem setup can be found in Figure 4.6. With this spring constant in place, the response of the system fits well within the parameters of this experiment. The displacement was found to be 0.2475 inches with an initial displacement of -0.2815 inches. Also, the vibrational speed was found to be roughly 6 Hz. This displacement is still slightly above the targeted 0.1-0.2 inches. However, this allows for increased stimulation of the user.

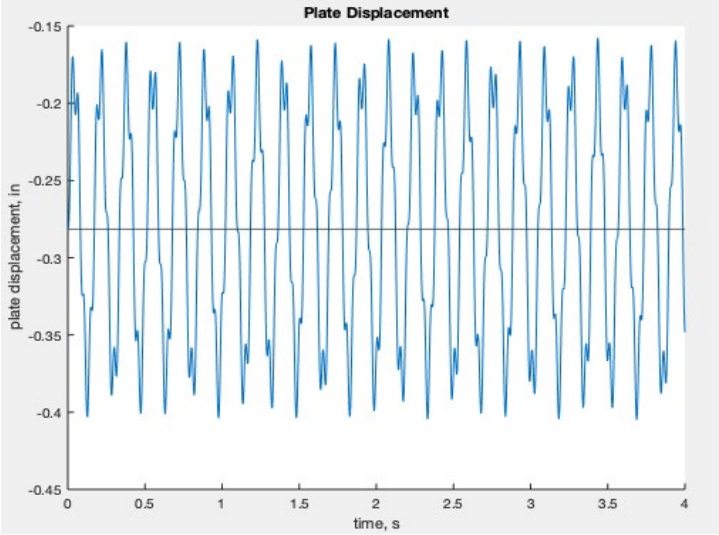

Figure 4.6: Final run of k=46.1 lb/in

One characteristic of note from these responses is the lack of smoothness of the sinusoidal curve. There are many jagged peaks along the path of the curve. These peaks and troughs are in response to the motor spinning faster than the plate is displacing. These individual smaller peaks correspond to moments when the eccentric mass is either at its peak or its trough concerning the direction of travel.

One parameter that will have a considerable effect on this response is the weight of the user. The heavier the user, the larger the initial displacement and the smaller the vibrational amplitude. For example, when the time responses of a 160lb user and a 190lb user are compared, these characteristics can be seen. This comparison can be seen in Figure. 4.7.

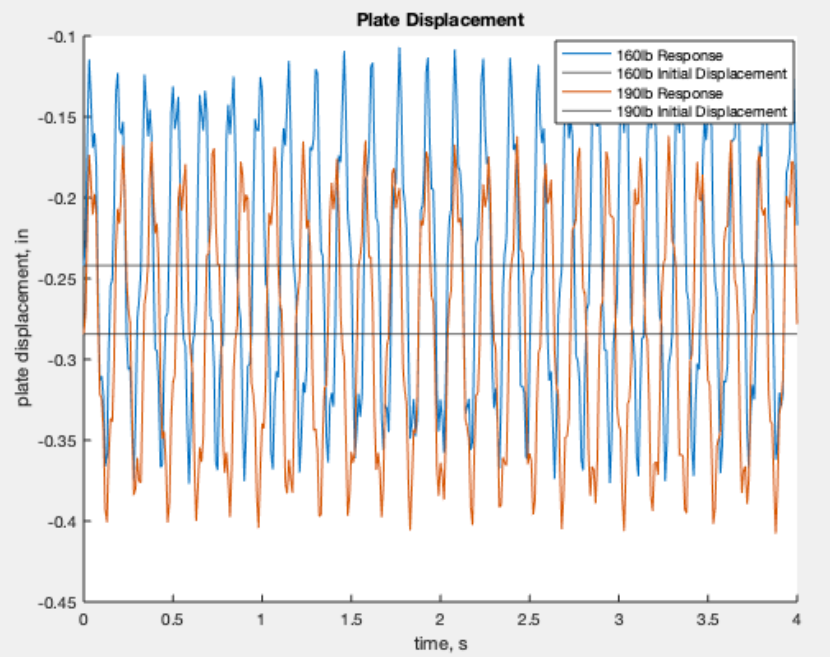

Figure 4.7: Response Comparison Between a 160lb and 190lb User

The initial displacements for the two users are -0.2420 inches and -0.2843 inches respectively. Also, the vibrational displacements are 0.2701 inches and 0.2461 inches respectively. Following this relationship, the max weight of a user for this system to

achieve a displacement of 0.2 inches was found to be 264lbs. This increase in weight also drops the vibrational speed to roughly 5Hz.

However, even with a 264lbs user, this is the highest weight to initially dip into the 0.1-0.2-inch displacement requirement. To confirm this design will be effective for the average human, average male and average female, the initial displacement and the vibrational displacement can be found in Table 4.1.

Table 4.1: Displacement Response of Various Average Weights

Weight of User (lb)	Initial Displacement (in)	Displacement at 1550 RPM (in)
195.8 (Avg. Male)	-0.2925	0.2391
188 (Avg. Human)	-0.2815	0.2475
168.4 (Avg. Female)	-0.2539	0.2612

Due to the positive results achieved within the ODE45 simulation, the general closed-form solution of the displacement equation is needed.

4.4 Closed-Form Solution

To solve this system for the final equation of motion, the Laplace/Inverse Laplace transform must be used. When the Laplace transform of Eq. (28) is performed, the initial form of the solution is represented by Eq.(29). To find the transfer function of this system, this equation must be solved for Y(s) and the initial conditions for y(0) and $\dot{y}(0)$ must be used. The initial condition for y(0) is found by setting all of the derivatives and the motor force in Eq(28) to zero and solving for y. This initial condition can be found in Eq.(30). The simplified transfer function (Y(s)) can be found in Eq.(31).

$$m_{total}[Y(s)s^2 - y(0)s - \dot{y}(0)] + n_{spring}kY(s) + \frac{m_{total}g}{s} = n_{ecc}(m_{ecc}r\omega^2)\frac{\omega}{s^2+\omega^2} \quad \text{Eq.(29)}$$

$$y(0) = \frac{-m_{total}g}{n_{spring}k} \quad \text{Eq.(30)}$$

$$Y(s) = \frac{\frac{-{m_{total}}^2 g}{n_{springs}k}s^4 + \left(-\frac{{m_{total}}^2 g\omega^2}{n_{springs}k} - m_{total}g\right)s^2 + (n_{ecc}m_{ecc}r\omega^3)s - m_{total}g\omega^2}{m_{total}s^5 + \left(n_{springs}k + M_{total}\omega^2\right)s^3 + n_{springs}k\omega^2 s} \quad \text{Eq.(31)}$$

When the assigned values are substituted into this equation the transfer function of the system with a 188lb user can be extracted as Eq.(32). With this function, an inverse Laplace transform was performed to find the time response of the system in the y direction. This equation is found to be Eq.(33) in feet and Eq.(34) in inches.

$$Y(s) = \frac{-0.1067s^4 - 2961.69s^2 + 38849.63s - 3977004.697}{4.692s^5 + 130247.67s^3 + 174898498.4s} \quad \text{Eq.(32)}$$

$$y(t)[ft] = (1.93x10^{-7})\cos(37.62t) + 0.00883\sin(37.62t) - (3.65x10^{-6})\cos(162.3t) - 0.00205\sin(162.3t) - 0.0227 \quad \text{Eq.(33)}$$

$$y(t)[in] = (2.317x10^{-6})\cos(37.62t) + 0.106\sin(37.62t) - (4.380x10^{-5})\cos(162.3t) - 0.025\sin(162.3t) - 0.273 \quad \text{Eq.(34)}$$

To test the precision between this equation and the response found in Figure 4.5, this response is graphed alongside the ODE45 response. This comparison can be found in Figure 4.8.

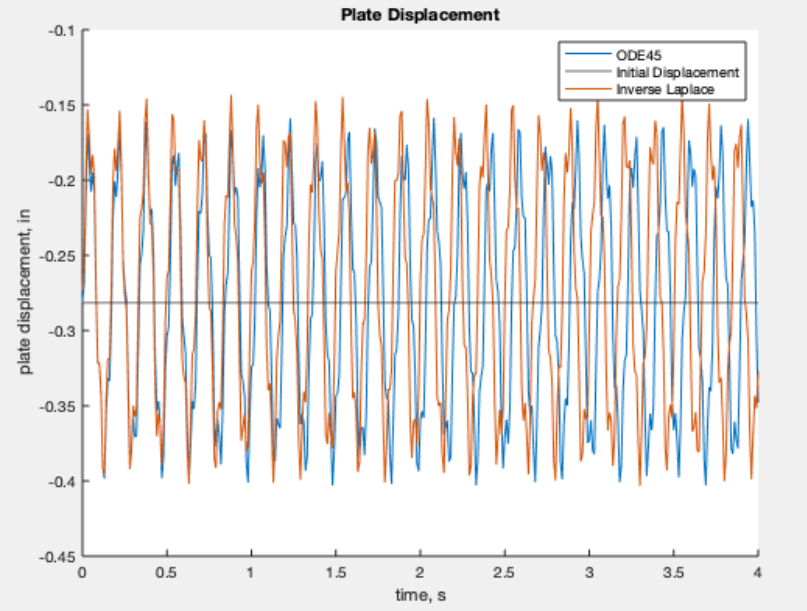

Figure 4.8: Inverse Laplace Response vs ODE45 Response

The overall displacement of the inverse Laplace solution is found to 0.26 inches which represents a roughly 5% difference from that of the ODE45 response (0.2475 inches). The physical response varies slightly in the vibrational speed of the response. The Inverse Laplace response is vibrating at a slightly faster speed. This causes an increasing difference in the response over time between the two solutions. This percent difference in time can be seen in Figure 4.9. This growing difference can be attributed to the decimal place kept through the calculation through the calculation of the Inverse Laplace solution and to the accuracy kept by the MATLAB software while running the ODE45 solution. It is expected that this percent difference between two sinusoids of roughly the same amplitude but of slightly different frequencies would rise over a certain period and then start to drop.

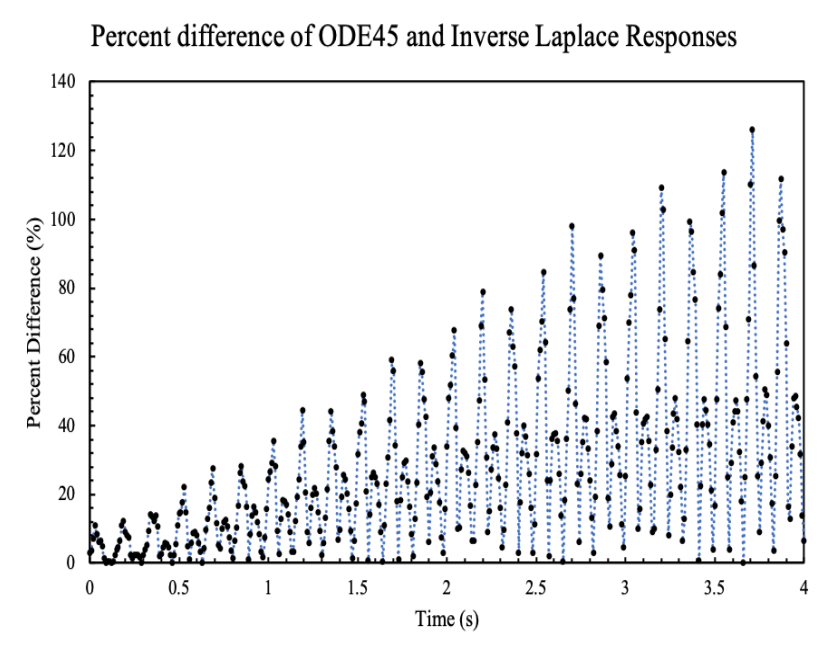

Figure 4.9: Percent Difference Over Time of the ODE45 and Inverse Laplace Responses

It will exhibit an overall sinusoidal behavior of itself due to the percent difference growing until the two sinusoids are offset by π and then the percent difference should decrease until realigned. This relationship will repeat continually. This continual relationship can be seen in Appx E.

CHAPTER 5

CONCLUSION

To evaluate the design of a simple spring, mass, motor design, a few steps must be taken and evaluated individually. First, the system must be set up in a Free-Body Diagram form to find the equations of the system and how it relates to various inputs. Next, these equations must be solved for the time response using a mathematical solver, such as the Laplace and inverse Laplace transform, or by using a computational tool such as ODE45 within MATLAB. These two solving methods effectively work to do the same thing, find the time response of an ordinary differential equation. When this is performed in the case of the design comprised of a Delrin plastic sheet, 12 springs, 4 linear bearings, an ERM motor and a user of 188 lbs the vibrational amplitude of the ODE45 solving method is found to be 0.2475 inches. The ODE45 simulation was also used to find the values of various parameters including the number of springs needed, the spring constant, the size of the eccentric mass and the value of the eccentricity needed to achieve the 0.1-0.2-inch displacement. When the same design is analyzed using by-hand solving methods, the vibrational amplitude is found to be 0.2600 inches. This relates to a 5% difference between the two solving methods. However, 5% relates to an almost unnoticeable tactile difference of 0.0125 inches of displacement. Thusly, these two solving methods represent two tactilely equal solutions.

APPENDIX A

EXAMPLE MASS/SPRING/DAMPER QUESTION

Initial Problem Setup and Free Body Diagram

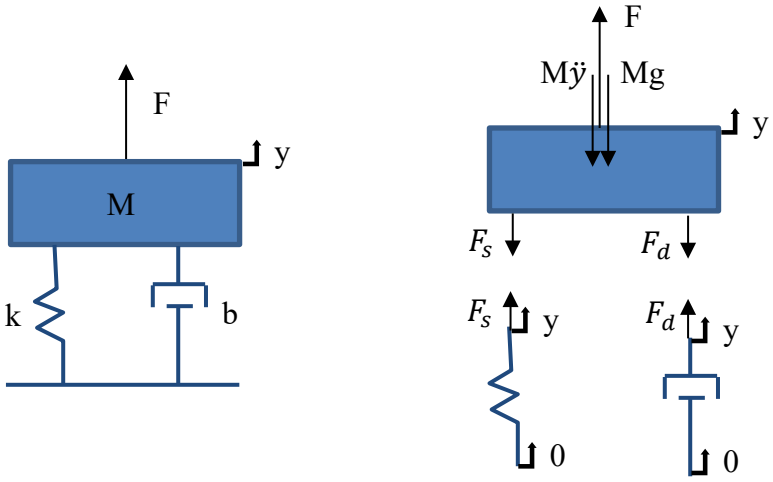

Equations of Each Force Balance

$$F_s = k(y - 0) = ky$$

$$F_d = b(\dot{y} - 0) = b\dot{y}$$

$$M\ddot{y} + Mg + F_s + F_d = F$$

$$M\ddot{y} + b\dot{y} + ky + Mg = F$$

Solution of y(0-)

At t=0, all derivatives are zero and no Force is acting on the system

$$M\ddot{y} + b\dot{y} + ky + Mg = F$$

0 0 0

$$y(0-) = \frac{-Mg}{k}$$

Laplace the Total Force Balance on the Mass

$$M\left(s^2Y(s) - sy(0-) - \dot{y}(0-)\right) + b(sY(s) - y(0-)) + kY(s) + \frac{Mg}{s} = \frac{F}{s}$$

$$Ms^2Y(s) - Msy(0-) - M\dot{y}(0-) + bsY(s) - by(0-) + kY(s) + \frac{Mg}{s} = \frac{F}{s}$$

$$Ms^2Y(s) + bsY(s) + kY(s) = \frac{F}{s} - \frac{Mg}{s} + Msy(0-) + M\dot{y}(0-) + by(0-)$$

$$Y(s)(Ms^2 + bs + k) = \frac{Ms^2y(0-) + \big(M\dot{y}(0-) + by(0-)\big)s + (F - Mg)}{s}$$

$$Y(s) = \frac{Ms^2y(0-) + \big(M\dot{y}(0-) + by(0-)\big)s + (F - Mg)}{Ms^3 + bs^2 + ks}$$

Using the values for g, M, F, k, b, y(0-) and $\dot{y}(0-)$. Solve for Y(s).

g = 32.174 $\frac{ft}{s^2}$

F = 40 lb

M = 6 lb

k = 10 $\frac{lb}{ft}$

b = 16 $\frac{lb*s}{ft}$

y(0-) = $\frac{-Mg}{k} = -19.644\ ft$

$$\dot{y}(0-) = 0$$

$$Y(s) = \frac{6(-19.644)s^2 + 16(-19.644)s + (40 - 6(32.174))}{6s^3 + 16s^2 + 10s}$$

$$Y(s) = \frac{-115.8264s^2 - 308.87s - 153.044}{6s^3 + 16s^2 + 10s}$$

Find the Roots of the Denominator

$$6s^3 + 16s^2 + 10s = s(6s^2 + 16s + 10)$$

$$\frac{-b \pm \sqrt{b^2 - 4ac}}{2a} = \frac{-16 \pm \sqrt{16^2 - 4(6)(10)}}{2(6)} = \frac{-16 \pm \sqrt{16}}{12} = -1\ and\ -\frac{5}{3}$$

Therefore s = 0, -1 and $-\frac{5}{3}$.

$$Y(s) = \frac{-115.8264s^2 - 308.87s - 153.044}{s(s+1)(s+\frac{5}{3})}$$

Perform Partial Fraction Decomposition

$$Y(s) = \frac{-115.8264s^2 - 308.87s - 153.044}{s(s+1)(s+\frac{5}{3})} = \frac{K1}{s} + \frac{K2}{s+1} + \frac{K3}{s+\frac{5}{3}}$$

$$K1 = s(Y(s))|_{s=0} = -91.83$$

$$K2 = (s+1)(Y(s))|_{s=-1} = -59.99$$

$$K3 = (s+\frac{5}{3})(Y(s))\Big|_{s=-\frac{5}{3}} = 35.99$$

$$Y(s) = -\frac{91.83}{s} - \frac{59.99}{s+1} + \frac{35.99}{s+\frac{5}{3}}$$

Inverse Laplace Y(s) to find the time domain function y(t)

$$\mathcal{L}^{-1}\left[-\frac{91.83}{s}\right] = -91.83$$

$$\mathcal{L}^{-1}\left[-\frac{59.99}{s+1}\right] = -59.99e^{-t}$$

$$\mathcal{L}^{-1}\left[\frac{35.99}{s+\frac{5}{3}}\right] = 35.99e^{-\frac{5}{3}t}$$

$$y(t) = \mathcal{L}^{-1}[Y(s)] = -91.83 - 59.99e^{-t} + 35.99e^{-\frac{5}{3}t}$$

MATLAB Code to receive the time response using ode45

```
function SMD_Example

clc
clear all

g = 32.174;     %ft/s^2
m = 6; %lbm
k = 10; %(lbf/ft) Spring constant
b = 16; %lbf*s/ft Dampening Coefficient
F = 40; %lbf

yo = ((-m*g)/(k)) %initial y-position at equilibrium
```

```
%solving the differential equation for the displacement response
[t,y] = ode45(@Eqns2,[0 8],[yo 0]);
y=y(:,1); %isolates the displacement response

%plotting displacement vs time and a constant y value of
equilibrium
%displacement
figure(2)
hold on
plot(t,y)
xlabel('time, s');
ylabel('mass displacement, in');
title('Mass displacement over time');
hold off

%solving the differential equation for displacement and setting
up the
%system variables
    function dy = Eqns2(t,y)
        dy=zeros(2,1);

        disp=y(1); %displacement of the mass

        dy(1)= y(2); %velocity of the mass
        dy(2) = -g-(k*y(1)/m)-(b*dy(1)/m)+(F/m); %acceleration of
the mass

    end
end
```

MATLAB Output

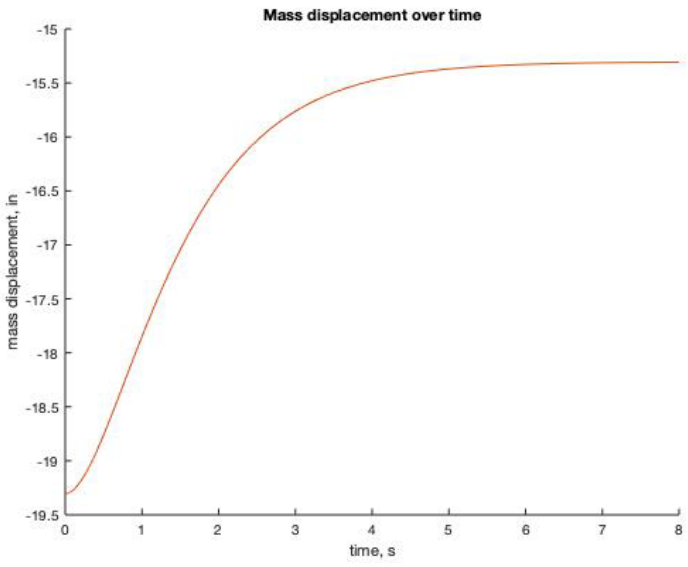

APPENDIX B

MATLAB CODE AND OUTPUT FOR THE VIBRATIONAL PLATFORM

MATLAB Code

```
function SENIOR_DESIGN_1

clc
clear all

distrib = 0.78; %percent of weight on seat from study
Wuser = 188*distrib;    %(lbf) average weight of user
Wmotor = 11.2;   %(lbf) weight of motor based on amazon posting
Wsheet = 1.25;  %(lbf) weight of ABS sheet from solidworks model
Wpin = 0.16;    %(lbf) weight of the bearing pins
WpinC = 0.05;   %(lbf) weight of the connectors between the pin
and the ABS sheet
WmotorC = 0; %(lbf) weight of the connectors between the motor
and the ABS Sheet
Wecc = 2.1;   %(lbf) weight of single eccentric mass from
solidworks. cast iron
g = 32.174;    %ft/s^2
necc = 2; %number of eccentric masses
nPin = 4;   %number of pins used to linearize the motion of the
system
nspring = 12;   %number of springs used

muser = Wuser/g;   %(lbm)
mmotor = Wmotor/g;  %(lbm)
msheet = Wsheet/g;  %(lbm)
mpin = Wpin/g;    %(lbm)
mpinC = WpinC/g;   %(lbm)
%mmotorC = WmotorC/g; %(lbm)
mecc = Wecc/g; %(lbm)

%(lbm) total mass of system: plate, user, connectors, pins and
motors with the eccentric masses removed due to being the input
force
mtot = nPin*(mpin+mpinC) + msheet + (((mmotor) - necc*mecc))+
muser;

k = 46.1*12;  %(lbf/ft) Spring constant
r = 0.8/12;   %(ft) eccentricity (distance between rod and center
of mass) found using solidworks (cast iron) and dimensions from
amazon posting
RPM = 1550; %rated RPM between 12V/4000RPM and 24V/8000RPM
w = (2*pi*RPM/60);  %(rad/s) angular velocity of the rotating
mass
Fo = necc*(mecc*r*(w^2)); %(lbf) force of rotating eccentric mass
yo1 = ((-mtot*g)/(nspring*k)); %(ft) initial y-position at
equilibrium
yo2 = yo1*12 %(in) initial y-position in inches

%solving the differential equation for the displacement response
```

```
[t,y] = ode45(@Eqns2,[0:0.01:4],[yo1 0]);
y=y(:,1); %isolates the displacement response

ymax = max(y)*12; %(in) max peak value of the oscillation
ymin = min(y)*12; %(in) min peak value of the oscillation
dy = abs(ymin)-abs(ymax) %(in) displacement of oscillation
ymin = abs(ymin); %(in) lowest point reached by plate
wn = sqrt((nspring*k)/mtot); %natural frequency of the system

%plotting displacement vs time and a constant y value of
equilibrium
%displacement
figure(2)
hold on
plot(t,y*12)
yline(yo2);
xlabel('time, s');
ylabel('plate displacement, in');
title('Plate Displacement');

hold off

%solving the differential equation for displacement and setting
up the
%system variables
    function dy = Eqns2(t,y)
        dy=zeros(2,1);

        disp=y(1); %displacement of the plate

        dy(1)= y(2); %velocity of the plate
        dy(2) = ((Fo*sin(w*t)) - (nspring*k*disp) -
(mtot*g))/mtot; %acceleration of the plate

    end


end
```

MATLAB OUTPUT

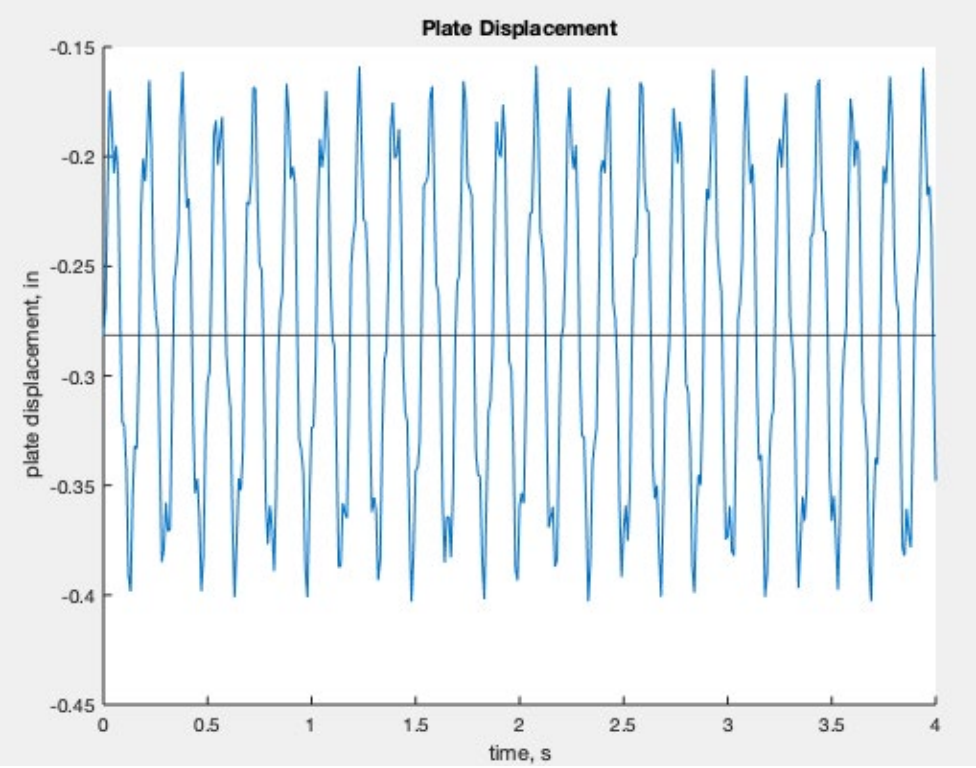

APPENDIX C

SOLUTION OF LAPLACE/INVERSE LAPLACE TRANSFORM

Laplace Transform

$$m_{total}\ddot{y} + n_{springs}ky + m_{total}g = n_{ecc}(m_{ecc}r\omega^2) * \sin(\omega t)$$

$$y(0) = \frac{-m_{total}g}{n_{spring}k}$$

$$\dot{y}(0) = 0$$

$$m_{total}[Y(s)s^2 - y(0)s - \dot{y}(0)] + n_{spring}kY(s) + \frac{m_{total}g}{s} = n_{ecc}(m_{ecc}r\omega^2)\frac{\omega}{s^2+\omega^2}$$

$$Y(s)\left[m_{total}s^2 + n_{spring}k\right] - m_{total}y(0)s - m_{total}\dot{y}(0) + \frac{m_{total}g}{s} = n_{ecc}(m_{ecc}r\omega^2)\frac{\omega}{s^2+\omega^2}$$

$$Y(s) = \frac{n_{ecc}(m_{ecc}r\omega^2)\frac{\omega}{s^2+\omega^2} + m_{total}y(0)s + m_{total}\dot{y}(0) - \frac{m_{total}g}{s}}{m_{total}s^2 + n_{spring}k}$$

$$Y(s) = \frac{n_{ecc}(m_{ecc}r\omega^2)\frac{\omega}{s^2+\omega^2} - \frac{{m_{total}}^2 g}{n_{spring}k}s - \frac{m_{total}g}{s}}{m_{total}s^2 + n_{spring}k}$$

$$Y(s) = \frac{\frac{-{m_{total}}^2 g}{n_{springs}k}s^4 + \left(-\frac{{m_{total}}^2 g\omega^2}{n_{springs}k} - m_{total}g\right)s^2 + (n_{ecc}m_{ecc}r\omega^3)s - m_{total}g\omega^2}{m_{total}s^5 + \left(n_{springs}k + M_{total}\omega^2\right)s^3 + n_{springs}k\omega^2 s}$$

$$m_{total} = n_{pin} * \left(m_{pin} + m_{pinC}\right) + m_{sheet} + \left((m_{motor} - n_{ecc} * m_{ecc} + m_{motorC})\right) + m_{user}$$

Substitute in all assigned values

$m_{user} = 4.415lbm$ $\quad$ $m_{pinC} = 0.00155lbm$ $\quad$ $m_{sheet} = 0.0388lbm$

$m_{motor} = 0.348lbm$ $\quad$ $m_{ecc} = 0.0681lbm$ $\quad$ $m_{pin} = 0.00497lbm$

$n_{spring} = 12$ $\quad$ $k = 46.1\frac{lbF}{in} = 553.2\frac{lbF}{ft}$ $\quad$ $\omega = \frac{2\pi RPM}{60} = 162.32\frac{rad}{s}$

$n_{pin} = 4$ $\quad$ $r = 0.067\ ft$ $\quad$ $g = 32.2\frac{ft}{s^2}$

$n_{ecc} = 2$ $\quad$ $RPM = 1550$

$$m_{total} = 4.69168\ lbm$$

$$Y(s) = \frac{-0.1067s^4 - 2961.69s^2 + 38849.63s - 3977004.697}{4.692s^5 + 130247.67s^3 + 174898498.4s}$$

Perform Inverse Laplace Transform using TI -nspire CX-CAS

$$y(t)[ft] = (1.93x10^{-7})\cos(37.62t) + 0.00883\sin(37.62t) - (3.65x10^{-6})\cos(162.3t)$$
$$-0.00205\sin(162.3t) - 0.0227$$

$$y(t)[in] = (2.317x10^{-6})\cos(37.62t) + 0.106\sin(37.62t) - (4.380x10^{-5})\cos(162.3t)$$
$$-0.025\sin(162.3t) - 0.273$$

APPENDIX D

GRAPHING THE INVERSE LAPLACE SOLUTION

MATLAB Code

```
clc
clear all

m = 4.69168;
g = 32.174;
Ns = 12;
k = 46.1*12;
RPM = 1550;
w = (2*pi()*RPM)/60;
Me = 0.0681;
r = 0.8/12;


num = [((-(m^2)*g)/(Ns*k)) 0 (((-(m^2)*g*(w^2))/(Ns*k))-(m*g))
2*Me*r*(w^3) -m*g*(w^2)];
den = [m 0 (Ns*k)+(m*(w^2)) 0 Ns*k*(w^2) 0];

num = [-0.0226 0 -631.265 8280.537 -847671.7715];
den = [1 0 27761.414 0 37278437.23 0];

G = tf(num, den)

t = 0:0.01:4;

y2 = (((2.317E-6)*cos(37.62*t)) + (0.10596*sin(37.62*t)) -
((4.3796E-5)*cos(162.316*t)) - (0.024552*sin(162.316*t))-
0.272868);
disp2 = abs(max(y2)-min(y2))
figure(2)
plot(t,y2)
xlabel('time, s');
ylabel('plate displacement, in');
title('Plate Displacement');
```

MATLAB Output

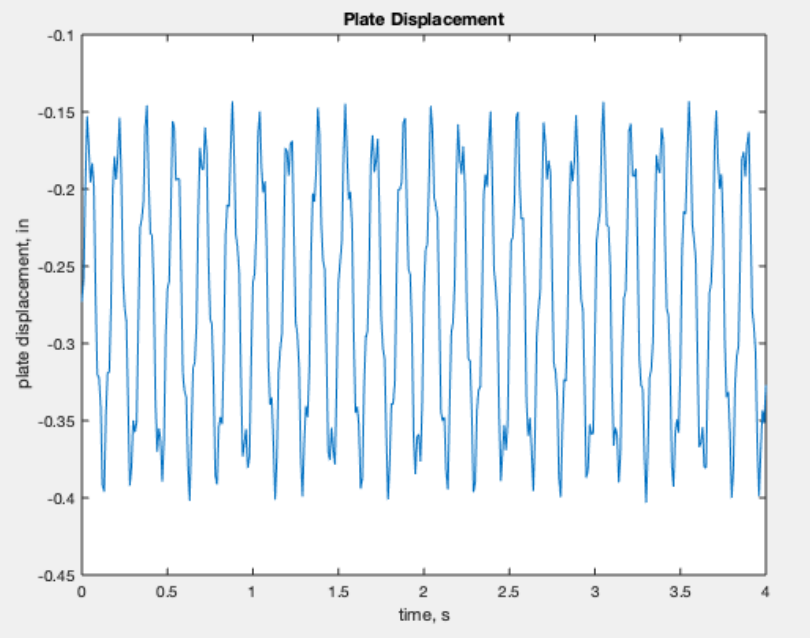

APPENDIX E

COMPARISON BETWEEN ODE45 AND INVERSE LAPLACE RESPONSE

Y-response of the ODE45 and Inverse Laplace results from t=0 to t=50s

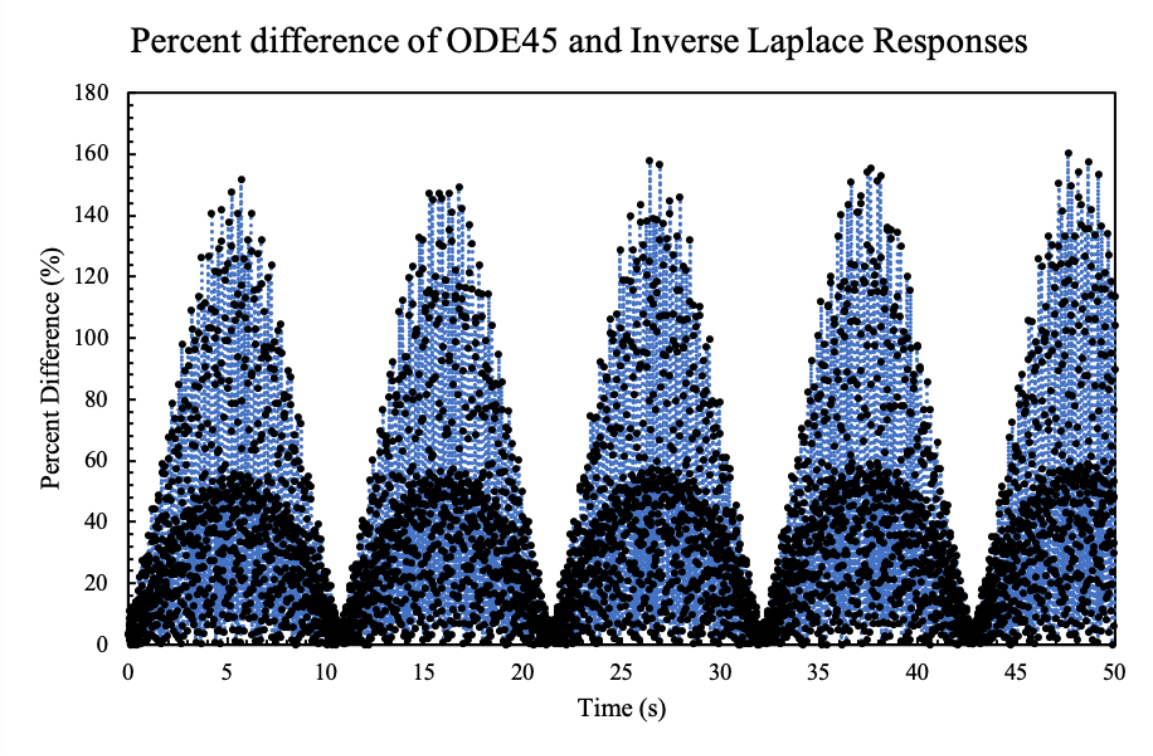

REFERENCES

AB-004 : Understanding ERM Vibration Motor Characteristics. (n.d.). Retrieved February 14, 2020, from https://www.precisionmicrodrives.com/content/ab-004-understanding-erm-vibration-motor-characteristics/

AB-020 : Understanding Linear Resonant Actuator Characteristics. (n.d.). Retrieved February 15, 2020, from https://www.precisionmicrodrives.com/content/ab-020-understanding-linear-resonant-actuator-characteristics/

Ahmed, W. K. (2013). Advantages and Disadvantages of Using MATLAB/ode45 for Solving Differential Equations in Engineering Applications. *International Journal of Engineering*, *7*(1), 25–31. Retrieved from http://www.cscjournals.org/

Cohen, D.E. (2018). *U.S. Patent No. 9,949,004*. Washington, DC: U.S. Patent and Trademark Office.

Dawkins, P. (2018, June 3). Inverse Laplace Transforms. Retrieved February 19, 2020, from http://tutorial.math.lamar.edu/Classes/DE/InverseTransforms.aspx

Fryer, C.D., Kruszon-Moran, D., Gu, Q., Ogden, C. L. (2018). Mean Body Weight, Height, Waist Circumference, and Body Mass Index Among Adults: United States, 1999-2000 Through 2015-2016. *Health Statistics Reports*, 122. Retrieved from cdc.gov.

Hullender, D. (2018). *Dynamic Systems Modeling and Simulation: Theory and Examples* (17th ed.).

Inverse Laplace Transform. (n.d.). Retrieved February 23, 2020, from https://www.sciencedirect.com/topics/engineering/inverse-laplace-transform

Laplace Transforms. (n.d.). Retrieved February 20, 2020, from https://www.sciencedirect.com/topics/engineering/laplace-transforms

Linear Actuators 101 - Everything you need to know about a linear Actuator. (2018, November 16). Retrieved February 15, 2020, from https://www.firgelliauto.com/blogs/news/linear-actuators-101

Nise, N.S. (2015). *Control Systems Engineering* (7th ed.). Wiley.

Norton, R.L. (2011). *Machine Design: An Integrated Approach* (4th ed.). Prentice-Hall.

ode45. (n.d.). Retrieved February 22, 2020, from https://www.mathworks.com/help/matlab/ref/ode45.html

ode45 - Differential Equation Solver. (n.d.). Retrieved February 24, 2020, from https://www.math.purdue.edu/academic/files/courses/2005spring/MA266/ode45.pdf

Oser, R.B., & Long, S. (2011). *U.S. Patent No. 8,077,884*. Washington, DC: U.S. Patent and Trademark Office.

Senan, N. A. F. (n.d.). A brief introduction to using ode45 in MATLAB. Retrieved February 26, 2020, from http://www.eng.auburn.edu/~tplacek/courses/3600/ode45berkley.pdf

Smith, J. O. (2007, September). Plotting Complex Sinusoids as Circular Motion. Retrieved February 12, 2020, from https://ccrma.stanford.edu/~jos/filters/Plotting_Complex_Sinusoids_Circular.html

Stress Management For The Soul. (n.d.). Retrieved March 5, 2020, from https://www.sosoundsolutions.com/

The SolTec®Lounge. (n.d.). Retrieved March 4, 2020, from https://solteclounge.com/

The BodySound Chair. (n.d.). Retrieved March 4, 2020, from http://www.thebodysoundchair.com/

BIOGRAPHICAL INFORMATION

Lukas Willingham returned to school, after working within the Advertising field for 3.5 years, to earn an Honors Bachelor of Science in Mechanical Engineering, with a minor in Aerospace Engineering, from The University of Texas at Arlington. He worked on a variety of projects while attending school, including a 3D printed sinusoid drawing device and a cooling system for a silicon chip. The 3D printed sinusoid drawing device utilized a gear previously used within sprinklers to draw two speeds of sinusoid using the same device. He is working towards a position in the Mechanical Engineering design field with a passion for Aerospace advancement. Lukas currently lives in Ft. Worth, Texas with his wife and two Siberian Huskies (Sterling and Remus).